




Spin-orbital correlations in the two-orbital Hubbard model

Alfonso Romano^{1,2}, Delia Guerra¹, Filomena Forte², Canio Noce^{1,2,a} 

¹ Dipartimento di Fisica “E.R. Caianiello”, Università degli Studi di Salerno, 84084 Fisciano, SA, Italy

² CNR-SPIN, UOS di Salerno, 84084 Fisciano, SA, Italy

Received: 14 November 2022 / Accepted: 2 May 2023

© The Author(s) 2023

Abstract We use exact diagonalization results to investigate how the ground state of a two-site, two-orbital Hubbard model evolves in terms of the crystal field energy and a magnetic spin symmetry breaking field. We show that, based on the behavior of a properly defined composite spin-orbital correlation function, the different regions of the related phase diagrams can be classified according to the extent to which spin and orbital degrees of freedom turn out to be correlated.

1 Introduction

Correlated electron systems exhibit a large variety of peculiar properties, often leading to substantial deviations from the predictions of the conventional band theory [1–3]. Phenomena such as the metal-insulator transition driven by given external agents (temperature, pressure, etc.) or the development of magnetic orders in specific classes of solids, are typical manifestations of the failure of descriptions where electron–electron interaction is neglected. The strong interplay between charge, spin and orbital degrees of freedom that usually accompanies strong electronic correlations gives rise to these phenomena in fundamental classes of materials, such as in particular transition metal compounds, and can only be analysed within the framework of correlated electron models such as the Hubbard model and extensions of it.

In recent years, the intricate charge-spin-orbital interplay that characterizes the phenomenology of several materials has often been treated as a possible manifestation of quantum entanglement [4–6], i.e. of specific correlations which prevent a quantum eigenstate from being represented as a product of states belonging to distinct subspaces of the full Hilbert space. Great efforts have been made to investigate this topic in the framework of condensed matter physics, mostly focused on models of interacting spin chains [7–9], also in view of their possible application to quantum computation. Nonetheless, the search for entangled states has rapidly been extended to other solid-state systems. Quantum phase transitions, spin disorder, Kondo effect, many-body localization are examples of phenomena which have been successfully reconsidered from this point of view [7–11]. More recently, great attention has been devoted to the entanglement involving spin and orbital degrees of freedom in transition metal oxides [4–6], mostly investigated within the well-known Kugel-Khomskii model [12]. In compounds with active orbital degrees of freedom, spin-orbital superexchange can be induced by strong Coulomb interactions tending to localize electrons. Experimental results requiring for their explanation the assumption of a significative spin-orbital entanglement have been repeatedly obtained in the last years, especially in vanadium perovskites. A list of recent papers where these results are shown and discussed can be found in Ref.[5].

With the aim of shedding light on the physics of the above-mentioned systems, we focus here on the spin/orbital correlations that may develop into a two-orbital extended Hubbard model. To this end, we will take advantage from a recent exact diagonalization study of the two-site, two-orbital Hubbard model, where the spin and the pseudospin orbital symmetries have been fully taken into account [13]. Here we consider an extension of this model, including an external spin-symmetry breaking magnetic field, together with a splitting of the orbital site energies simulating the effect of a crystal field. How the ground state varies as a function of these two quantities is presented, for fixed choices of the model parameters, in phase diagrams where the different regions are identified by the values of the total spin and pseudospin quantum numbers. The possible presence in each of these regions of quantum correlations between spin and orbital degrees of freedom is then determined by evaluating the behavior of a suitably defined spin-orbital correlator. Following this approach, we conclude that the magnetic field and the crystal field splitting can both separately represent efficient quantum tools to control whether the quantum states are entangled, in the sense that spin and orbital degrees of freedom cannot be separated. Conversely, we find out that a suitable tuning of the crystal field potential and/or the magnetic external field drives the system in fully polarized configurations with a vanishing degree of spin-orbital correlation.

Alfonso Romano, Delia Guerra, Filomena Forte and Canio Noce have contributed equally to this work.

^a e-mail: cnoce@unisa.it (corresponding author)

We point out that our results have been obtained within an approach where the microscopic interactions included in the model are treated on equal footing in an exact way. Furthermore, we consider the case of spin-orbital correlations resulting from on-site Coulomb interactions only, while we do not take into account possible effects arising from on-site spin-orbit coupling, as it is usually done in studies of transition metal compounds with partially filled $4d$ and $5d$ orbitals [6]. The results presented here should thus be referred to systems with partially filled $3d$ orbitals where spin-orbit coupling can be considered negligible.

2 Model and symmetries

We consider strongly correlated electrons on a lattice with two different orbitals on each site, in the presence of an external magnetic field. The corresponding Hamiltonian is

$$H = H_0 + H_I, \quad (1)$$

where the non-interacting part H_0 includes site energies and electron hopping between non-degenerate orbitals of the same type on nearest-neighbour sites, in the presence of a magnetic field:

$$H_0 = \sum_{i,\sigma} \left(\epsilon_1 c_{i1\sigma}^\dagger c_{i1\sigma} + \epsilon_2 c_{i2\sigma}^\dagger c_{i2\sigma} \right) - t \sum_{\langle ij \rangle, \alpha, \sigma} c_{i\alpha\sigma}^\dagger c_{j\alpha\sigma} + \sum_{i,\alpha} h \left(c_{i\alpha\uparrow}^\dagger c_{i\alpha\uparrow} - c_{i\alpha\downarrow}^\dagger c_{i\alpha\downarrow} \right). \quad (2)$$

Here $c_{j\alpha\sigma}^\dagger$ is the creation operator for an electron with spin σ at site i in the α orbital ($\alpha = 1, 2$), t is the hopping amplitude, h represents the external magnetic field. We denote the difference between the onsite energy of the two orbitals at each site by $\Delta = \epsilon_2 - \epsilon_1$.

The electron–electron interaction is described by the operator H_I [14–17],

$$H_I = (U + J) \sum_{i,\alpha} n_{i\alpha\uparrow} n_{i\alpha\downarrow} + U \sum_{i,\sigma} n_{i1\sigma} n_{i2\bar{\sigma}} + (U - J) \sum_{i,\sigma} n_{i1\sigma} n_{i2\sigma} + J \sum_{i,\sigma} c_{i1\sigma}^\dagger c_{i2\bar{\sigma}}^\dagger c_{i1\bar{\sigma}} c_{i2\sigma}, \quad (3)$$

expressed in terms of the on-site Coulomb repulsion U and the Hund coupling J . We notice that H_I contains intra-site interactions only, distinguishing among the cases where electrons belonging to different orbitals have the same spin or opposite spins (here $\bar{\sigma} = -\sigma$). Moreover, with the above choice of the coupling constants, the total Hamiltonian is rotationally invariant with respect to the spin and the orbital degrees of freedom [18]. The condition $U > J$ is also assumed (with U and J being both positive), in order to ensure that the total interorbital interaction between electrons with the same spin is repulsive [19]. Throughout the paper all the energies are expressed in units of the hopping amplitude t and we assume $\epsilon_1 = 0$ as the reference energy.

Finally, we introduce the total spin and orbital pseudospin operators

$$\mathbf{S} = \frac{1}{2} \sum_{i,\sigma,\sigma',\alpha} c_{i\alpha\sigma}^\dagger (\boldsymbol{\sigma})_{\sigma\sigma'} c_{i\alpha\sigma'} \quad (4)$$

$$\mathbf{T} = \frac{1}{2} \sum_{i,\alpha,\alpha',\sigma} c_{i\alpha\sigma}^\dagger (\boldsymbol{\sigma})_{\alpha\alpha'} c_{i\alpha'\sigma}, \quad (5)$$

where $\boldsymbol{\sigma} \equiv (\sigma_x, \sigma_y, \sigma_z)$ is the vector having the Pauli matrices as components. We note that the model defined by Hamiltonian (1) exhibits two exact SU(2) symmetries, namely the SU(2) spin symmetry and the SU(2) pseudospin one.

3 Spin-orbital correlations

The possible occurrence of states with high values of the total spin S or pseudospin T quantum numbers, denoting the tendency of the system to show magnetic or orbital polarization, respectively, is here investigated in the case of half filling ($N = 4$). Hamiltonian (1) commutes with the mutually commuting operators $\{S^2, S_z, T^2, T_z\}$, implying that H can be cast in the form of a block diagonal matrix, where each block H_{S,S_z,T,T_z} is the projection in the subspace spanned by the vector states with the corresponding eigenvalues of the \mathbf{S} and \mathbf{T} operators [13, 20, 21]. The aforementioned matrix representation of H for $N = 4$ is reported in “Appendix.”

The ground state energy can thus be obtained in an analytical form via diagonalization of each block, and its evolution upon variations of the applied magnetic field h and the site energy separation Δ is shown in the phase diagrams of Fig. 1 for several

choices of the microscopic parameters U and J . The eigenenergies E_1 , E_2 and E_3 are associated with the subspaces $\{2, 2, 0, 0\}$, $\{0, 0, 2, 2\}$ and $\{1, 1, 1, 1\}$, respectively, and are given by [13]

$$E_1 = 2U - 2J - 2h \quad (6)$$

$$E_2 = 2U + 2J - 2\Delta \quad (7)$$

$$E_3 = \frac{1}{2} \left(5U + \sqrt{U^2 + 16t^2} - h - \Delta \right). \quad (8)$$

The corresponding eigenstates are

$$|1\rangle = |\uparrow, \uparrow, \uparrow, \uparrow\rangle \quad (9)$$

$$|2\rangle = |\uparrow\downarrow, 0, \uparrow\downarrow, 0\rangle \quad (10)$$

$$|3\rangle = A^{(3)} [|\uparrow, \uparrow, \uparrow\downarrow, 0\rangle - |\uparrow\downarrow, 0, \uparrow, \uparrow\rangle - C^{(3)} (|\uparrow\downarrow, \uparrow, \uparrow, 0\rangle + |\uparrow, 0, \uparrow\downarrow, \uparrow\rangle)], \quad (11)$$

where

$$A^{(3)} = \left[2 + 2(C^{(3)})^2 \right]^{-1/2} \quad (12)$$

$$C^{(3)} = \frac{2t}{E_3 - 3U}. \quad (13)$$

Finally, the eigenenergies E_4 and E_5 are associated with the subspaces $\{0, 0, 0, 0\}$ and $\{1, 1, 0, 0\}$, respectively. The analytical form of the corresponding eigenstates $|4\rangle$ and $|5\rangle$ is obtained from the diagonalization of the matrices $H_{0,0,0,0}$ and $H_{1,1,0,0}$ defined in Appendix.

4 Results

As expected, we find that for low values of h and Δ the ground state is the eigenstate $|4\rangle$, with the corresponding region of the phase diagram tending to shrink as increasing values of the correlation energy U are considered (see Fig. 1, upper and middle panels). Larger values of h , with Δ kept low, drive the system in the region where the ground state is the high-spin state $|1\rangle$, whereas in a specular way the increase of Δ stabilizes the high- T eigenstate $|2\rangle$ as the ground state, for suitably low values of h . Intermediate comparable values of h and Δ give rise to a competition of the states $|1\rangle$ and $|2\rangle$ with the state $|3\rangle$, with zone boundaries defined by the ratios E_1/E_3 and E_2/E_3 , respectively. In particular, the boundary between the two regions with ground states $|1\rangle$ and $|3\rangle$ is defined by the condition

$$\Delta - h = 2J + \frac{U - \sqrt{U^2 + 16t^2}}{2} \quad (14)$$

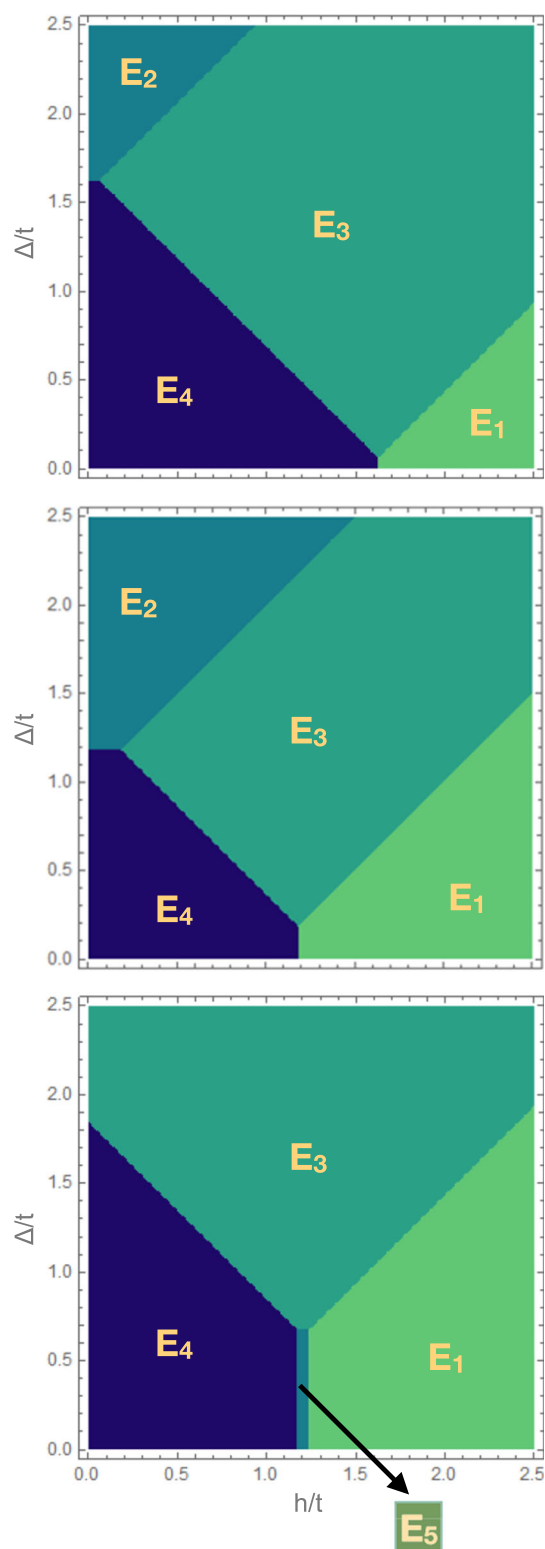
while the one between the regions with ground states $|2\rangle$ and $|3\rangle$ corresponds to

$$\Delta - h = 2J - \frac{U - \sqrt{U^2 + 16t^2}}{2}. \quad (15)$$

As a general trend, we see that increasing values of the correlation energy U tend to reduce the region where the eigenvalues of the total spin \mathbf{S} and of the total orbital operator \mathbf{T} are both non-vanishing, at the same time favouring the formation of a ground state where one of the two eigenvalues is maximized and the other is zero. In particular, the value of Δ for which there is an abrupt field-induced transition from $S = 0$ to $S = 2$ tends to enlarge as U is increased, with a similar behavior concerning the transition from $T = 0$ to $T = 2$ as Δ is increased at low h . Regarding the role played by the Hund coupling for a given value of U , one can clearly see from the lower panel of Fig. 1 that its increase tends to maximize the value of S , also leading to a reduction of the minimal field h required to have at low and moderate Δ a ground state with singly occupied orbitals with equal-spin electrons.

We also note that for $J = 0$ the phase diagram is symmetric along the diagonal $\Delta = h$ as a consequence of the complementary role played by Δ , as orbital symmetry-breaking field, and h , as spin symmetry-breaking field. Indeed, the unitary transformation $\mathbf{S} \longleftrightarrow \mathbf{T}$, together with $\Delta \longleftrightarrow h$, leaves unchanged the Hamiltonian, in this way giving rise to the symmetry discussed above. On the other hand, for finite values of J the spin-orbital symmetry is lost (see the lower panel of Fig. 1, showing the h - Δ phase diagram for $J = 0.5$). This of course was expected, given that the Hund coupling favours the high spin configurations, thus breaking the symmetry with respect to the counterpart represented by the orbital sector. In this case we also note that, due to the subtle interplay among the hopping and the interaction terms of the Hamiltonian, a new narrow region appears with ground state energy E_5 , characterized by an intermediate value of the spin quantum number, the orbital state being a singlet (i.e. $\{S = 1, S_z = 1, T = 0, T_z = 0\}$).

Fig. 1 Phase diagrams showing the ground state of the system as a function of the magnetic field h and the separation Δ between the orbital site energies, for $J = 0$ and $U = 1$ (upper panel), $J = 0$ and $U = 3$ (middle panel), $J = 0.5$ and $U = 1$ (lower panel). The energies E_1 , E_2 , E_3 , E_4 and E_5 correspond to states with $\{S = 2, S_z = 2, T = 0, T_z = 0\}$, $\{S = 0, S_z = 0, T = 2, T_z = 2\}$, $\{S = 1, S_z = 1, T = 1, T_z = 1\}$, $\{S = 0, S_z = 0, T = 0, T_z = 0\}$, and $\{S = 1, S_z = 1, T = 0, T_z = 0\}$, respectively. The boundary between two regions is determined from the crossing of the lowest eigenenergies in the two corresponding subspaces with different S and T

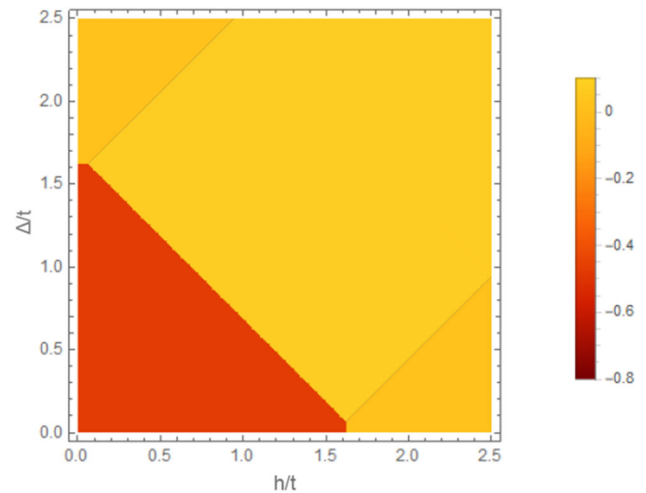


To gain a deeper physical understanding on the properties of the ground state of the system, we have investigated the intersite spin, orbital and spin-orbital correlation functions over the ground state, defined as follows, respectively [4]:

$$\hat{S} = \langle \mathbf{S}_1 \cdot \mathbf{S}_2 \rangle, \quad (16)$$

$$\hat{T} = \langle \mathbf{T}_1 \cdot \mathbf{T}_2 \rangle, \quad (17)$$

Fig. 2 Contour plot giving the value of the spin-orbital correlation function \hat{C} as a function of the magnetic field h and the separation Δ between the orbital site energies, for $J = 0$ and $U = 1$. The different regions are monochromatic because the magnitude of the correlator depends only on the ground state values of total spin S and total pseudospin T (the thin black lines only mark the boundary between the regions with a different shade of yellow)



$$\hat{C} = \langle (\mathbf{S}_1 \cdot \mathbf{S}_2)(\mathbf{T}_1 \cdot \mathbf{T}_2) \rangle - \langle \mathbf{S}_1 \cdot \mathbf{S}_2 \rangle \langle \mathbf{T}_1 \cdot \mathbf{T}_2 \rangle. \quad (18)$$

We note that the correlation function \hat{C} quantifies the average difference between the full spin-orbital operator and its decoupled product. Therefore, it gives information about the correlation between spin and orbital degrees of freedom. If $\hat{C} = 0$ the mean field decoupling of the spin and orbital operators is exact, and the spin and orbital channels may be treated independently from each other. Correspondingly, the ground-state wave function can be written as a product of its spin and orbital parts, separately. On the other hand, when $\hat{C} \neq 0$ the system is described by means of a state vector that cannot be factorized. Therefore, this correlator can be used to determine whether the mean-field decoupling between the spin and orbital pseudospin degrees of freedom can be applied.

Furthermore, we believe that the essence of the spin-orbital correlations is satisfactorily captured by solving this simple model for two-orbital configurations. Indeed, as we will show below, even solving the model Hamiltonian of Eq. (1) on a small cluster we are able to find spin-orbital correlated states and non-trivial spin-orbital configurations, as well as ground state wave functions close to a total spin-orbital singlet, involving a linear combination of spin singlet/high orbital configuration and high spin configuration/orbital singlet states.

Let us start the analysis considering the spin-orbital phase diagram plotted in Fig. 2. This plot has been obtained considering the values assumed by \hat{C} , according to the related colour code. We may easily infer that at low spin and orbital quantum numbers, \hat{C} is different from zero, signalling a correlation between spin and orbital degrees of freedom. When Δ or h increases above a suitable threshold value, depending on the Coulomb repulsion U , \hat{C} goes to zero in the two regions of high values of h and low values of Δ , and high values of Δ and low values of h , respectively (see Fig. 2, referring to the case $U = 1$ and $J = 0$). These two regions actually coincide with those of the phase diagram reported in the upper panel of Fig. 1, corresponding to the ground states with $\{S = 2, S_z = 2, T = 0, T_z = 0\}$ and $\{S = 0, S_z = 0, T = 2, T_z = 2\}$ and energies E_1 and E_2 , respectively.

A slightly different situation occurs for values of h and Δ giving rise to a ground state $\{1, 1, 1, 1\}$ with energy E_3 . Here, the correlator \hat{C} is non-vanishing, though very small, as evidenced by the value of \hat{C} for intermediate values of h (see the upper panel of Fig. 3), suggesting that in this region spin and orbital degrees of freedom exhibit a very low degree of correlation. For a higher value of Δ the increase of h makes the system pass from the region with $S = T = 0$ to the one with $S = T = 1$, as signalled by a single jump of the correlator from a largely negative value to a vanishingly small one, occurring at the zone boundary between the two regions (see the middle panel of Fig. 3, where $\Delta = 1$).

The above discussion allows to conclude that the $S = T = 1$ region can be seen as a precursor of a spin-orbital disordered phase, differently from what happens in the remaining part of the h - Δ phase diagram. This behaviour is not qualitatively altered by larger values of U , the main difference being a shrinking of this region, in agreement with the evolution with U of the h - Δ phase diagrams reported in Fig. 1.

Finally, we note that the main conclusions drawn above also apply when the Hund coupling is different from zero. We only mention that the appearance of a narrow region where the ground-state quantum numbers are $S = 1$ and $T = 0$ (see the phase diagram in the lower panel of Fig. 1), reflects on the behaviour of the correlator \hat{C} , which, as one can see in the lower panel of Fig. 3, exhibits at low Δ and for a small range of h , a value which is intermediate between the ones characterizing the E_4 and the E_1 regions.

Fig. 3 The correlator \hat{C} as a function of the magnetic field h for $\Delta = 0.5$ and $J = 0$ (upper panel), $\Delta = 1$ and $J = 0$ (middle panel), $\Delta = 0.5$ and $J = 0.5$ (lower panel), in the case $U = 1$

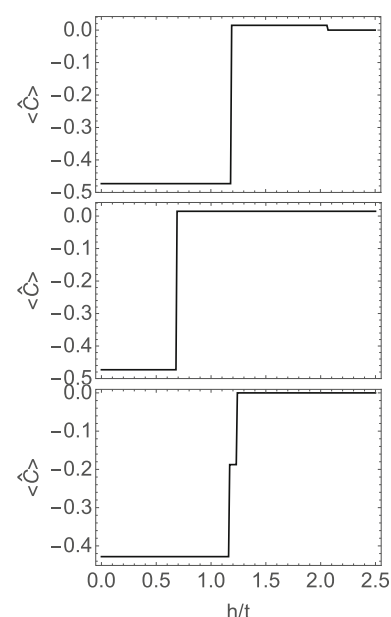
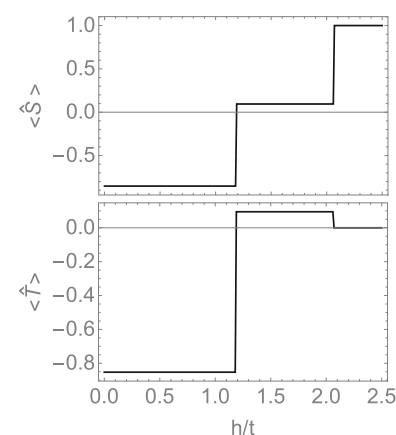


Fig. 4 The correlators \hat{S} (top panel) and \hat{T} (bottom panel) defined in the text, as functions of the magnetic field h for $\Delta = 0.5$, $J = 0$ and $U = 1$



5 Final remarks and conclusions

In conclusion, we have shown how an external magnetic field and/or an orbital energy splitting simulating a crystal field can drive significant spin-orbital correlations in a multi-orbital Hubbard model. This is done by looking at the behavior of a suitable spin-orbital correlation function which measures the extent to which spin and orbital degrees of freedom are decoupled. Our results suggest that two distinct experimental procedures allowing to control the degree of correlation in multi-orbital correlated systems are in principle available, based on the application of an external magnetic field or of a strain affecting the relative orbital site energies.

It is known that spin and orbital degrees of freedom may order in a complementary way, following the celebrated Goodenough–Kanamori rules [22–27]. These rules, derived long time ago from microscopic insights concerning the structure of the spin–orbital superexchange, predict that antiferromagnetic order coexists with ferro-orbital order and ferromagnetic order coexists with antiferro-orbital order. Importantly, they have been experimentally verified in many cases.

However, our results seem to contradict the Goodenough–Kanamori rules, since in the correlated regime both spin and orbital correlations have the same sign, as shown in Fig. 4, and the mean field decoupling procedure of spin and orbital operators fails so that the magnetic/orbital properties can be determined only by solving the fully correlated spin–orbital many-body problem. Nevertheless, in higher spin (orbital) state, the spin-orbital correlation is vanishing, implying that the mean field approximation may be applied, and since the orbital (spin) quantum number of the ground state is zero, the Goodenough–Kanamori rules would be verified.

Finally, we stress that these results can prove to be relevant in studies of transition metal oxides with more than six electrons to be accommodated in d -orbitals, in the case where the transition metal ion is in a tetragonal environment elongated enough to lead to a large separation of the lowest-lying t_{2g} states from the high-energy e_g ones. In this case the electron dynamics is dominated

by two spin-degenerate e_g orbitals, with no role played by the six electrons filling the t_{2g} triplet. Interestingly, in e_g orbitals the spin-orbit interaction is absent at the leading order [28], so that all the microscopic interactions determining the physical properties of the system are exactly the ones considered in our model.

Funding Open access funding provided by Università degli Studi di Salerno within the CRUI-CARE Agreement.

Data Availability Statement No Data associated in the manuscript.

Open Access This article is licensed under a Creative Commons Attribution 4.0 International License, which permits use, sharing, adaptation, distribution and reproduction in any medium or format, as long as you give appropriate credit to the original author(s) and the source, provide a link to the Creative Commons licence, and indicate if changes were made. The images or other third party material in this article are included in the article's Creative Commons licence, unless indicated otherwise in a credit line to the material. If material is not included in the article's Creative Commons licence and your intended use is not permitted by statutory regulation or exceeds the permitted use, you will need to obtain permission directly from the copyright holder. To view a copy of this licence, visit <http://creativecommons.org/licenses/by/4.0/>.

Appendix

The Hilbert space corresponding to $N = 4$ electrons has a dimension equal to 70. Using the fact that H commutes with the square of the spin and the pseudospin orbital operators, its matrix representation can be reduced into much smaller blocks having maximum size 6×6 . The eigenvalues and the corresponding eigenvectors can be derived diagonalizing the matrices reported below. They are denoted as H_{S^2, S_z, T^2, T_z} , according to the values assumed by the eigenvalues of the operators S^2 , S_z , T^2 , T_z , respectively:

$$\begin{aligned}
 H_{2,-2,0,0} &= 2(\Delta + h - J + U) \\
 H_{2,-1,0,0} &= 2\Delta + h - 2J + 2U \\
 H_{2,0,0,0} &= 2(\Delta - J + U) \\
 H_{2,1,0,0} &= 2\Delta - h - 2J + 2U \\
 H_{2,2,0,0} &= (\Delta - h - J + U) \\
 H_{0,0,2,-2} &= 2(J + U) \\
 H_{0,0,2,-1} &= \Delta + 2(J + U) \\
 H_{0,0,2,0} &= 2(\Delta + J + U) \\
 H_{0,0,2,1} &= 3\Delta + 2(J + U) \\
 H_{0,0,2,2} &= 2(2\Delta + J + U) \\
 H_{1,-1,1,-1} &= \begin{pmatrix} \Delta + h + 2U & 0 & -t & -t \\ 0 & \Delta + h + 2U & t & t \\ -t & t & \Delta + h + 3U & 0 \\ -t & t & 0 & \Delta + h + 3U \end{pmatrix} \\
 H_{1,0,1,-1} &= \begin{pmatrix} \Delta + 2U & 0 & -t & -t \\ 0 & \Delta + 2U & t & t \\ -t & t & \Delta + 3U & 0 \\ -t & t & 0 & \Delta + 3U \end{pmatrix} \\
 H_{1,1,1,-1} &= \begin{pmatrix} \Delta - h + 2U & 0 & -t & -t \\ 0 & \Delta - h + 2U & t & t \\ -t & t & \Delta - h + 3U & 0 \\ -t & t & 0 & \Delta - h + 3U \end{pmatrix} \\
 H_{1,-1,1,0} &= \begin{pmatrix} 2\Delta + h + 3U & \sqrt{\frac{2}{5}}t & 2\sqrt{\frac{2}{5}}t & 0 \\ \sqrt{\frac{2}{5}}t & 2\Delta + h + 2U & 0 & -\sqrt{\frac{2}{5}}t \\ 2\sqrt{\frac{2}{5}}t & 0 & 2\Delta + h + 2U & -2\sqrt{\frac{2}{5}}t \\ 0 & -\sqrt{\frac{2}{5}}t & -2\sqrt{\frac{2}{5}}t & 2\Delta + h + 3U \end{pmatrix}
 \end{aligned}$$

$$H_{1,0,1,0} = \begin{pmatrix} 2\Delta + 3U & 0 & \sqrt{2}t & 0 \\ 0 & 2(\Delta + U) & 0 & 0 \\ \sqrt{2}t & 0 & 2(\Delta + U) & -\sqrt{2}t \\ 0 & 0 & -\sqrt{2}t & 2\Delta + 3U \end{pmatrix}$$

$$H_{1,1,1,0} = \begin{pmatrix} 2\Delta - h + 3U & -\sqrt{\frac{2}{5}}t & -2\sqrt{\frac{2}{5}}t & 0 \\ -\sqrt{\frac{2}{5}}t & 2\Delta - h + 2U & 0 & \sqrt{\frac{2}{5}}t \\ -2\sqrt{\frac{2}{5}}t & 0 & 2\Delta - h + 2U & 2\sqrt{\frac{2}{5}}t \\ 0 & \sqrt{\frac{2}{5}}t & 2\sqrt{\frac{2}{5}}t & 2\Delta - h + 3U \end{pmatrix}$$

$$H_{1,-1,1,1} = \begin{pmatrix} 3\Delta + h + 2U & 0 & t & t \\ 0 & 3\Delta + h + 2U & -t & -t \\ t & -t & 3\Delta + h + 3U & 0 \\ t & -t & 0 & 3\Delta + h + 3U \end{pmatrix}$$

$$H_{1,0,1,1} = \begin{pmatrix} 3\Delta + 2U & 0 & t & t \\ 0 & 3\Delta + 2U & -t & -t \\ t & -t & 3\Delta + 3U & 0 \\ t & -t & 0 & 3\Delta + 3U \end{pmatrix}$$

$$H_{1,1,1,1} = \begin{pmatrix} 3\Delta - h + 2U & 0 & t & t \\ 0 & 3\Delta - h + 2U & -t & -t \\ t & -t & 3\Delta - h + 3U & 0 \\ t & -t & 0 & 3\Delta - h + 3U \end{pmatrix}$$

$$H_{1,-1,0,0} = \begin{pmatrix} 2\Delta + h + 3U & \sqrt{2}t & 0 \\ \sqrt{2}t & 2\Delta + h - 2J + 2U & \sqrt{2}t \\ 0 & \sqrt{2}t & 2\Delta + h + 3U \end{pmatrix}$$

$$H_{1,0,0,0} = \begin{pmatrix} 2\Delta + 3U & \sqrt{2}t & 0 \\ \sqrt{2}t & 2(\Delta - J + U) & \sqrt{2}t \\ 0 & \sqrt{2}t & 2\Delta + 3U \end{pmatrix}$$

$$H_{1,1,0,0} = \begin{pmatrix} 2\Delta - h + 3U & \sqrt{2}t & 0 \\ \sqrt{2}t & 2\Delta - h - 2J + 2U & \sqrt{2}t \\ 0 & \sqrt{2}t & 2\Delta - h + 3U \end{pmatrix}$$

$$H_{0,0,1,-1} = \begin{pmatrix} \Delta + 2(J + U) & \sqrt{2}t & -\sqrt{2}t \\ \sqrt{2}t & \Delta + 3U & 0 \\ -\sqrt{2}t & 0 & \Delta + 3U \end{pmatrix}$$

$$H_{0,0,1,0} = \begin{pmatrix} 2(\Delta + J + U) & -\sqrt{2}t & -\sqrt{2}t \\ -\sqrt{2}t & 2\Delta + 3U & 0 \\ -\sqrt{2}t & 0 & 2\Delta + 3U \end{pmatrix}$$

$$H_{0,0,1,1} = \begin{pmatrix} 3\Delta + 2(J + U) & \sqrt{2}t & -\sqrt{2}t \\ \sqrt{2}t & 3\Delta + 3U & 0 \\ -\sqrt{2}t & 0 & 3\Delta + 3U \end{pmatrix}$$

$$H_{0,0,0,0} = \begin{pmatrix} 2\Delta + \frac{8J}{5} + 2U & 0 & -\sqrt{\frac{6}{5}}t & -\frac{1}{5}(6J) & -\sqrt{\frac{6}{5}}t & 0 \\ 0 & 2(\Delta + 3U) & -2t & 0 & 0 & 0 \\ -\sqrt{\frac{6}{5}}t & -2t & 2\Delta + 3U & 2\sqrt{\frac{6}{5}}t & 0 & 0 \\ -\frac{1}{5}(6J) & 0 & 2\sqrt{\frac{6}{5}}t & 2\Delta - \frac{8J}{5} + 2U & 2\sqrt{\frac{6}{5}}t & 0 \\ -\sqrt{\frac{6}{5}}t & 0 & 0 & 2\sqrt{\frac{6}{5}}t & 2\Delta + 3U & -2t \\ 0 & 0 & 0 & 0 & -2t & 2(\Delta + 3U) \end{pmatrix}$$

References

1. P. Fazekas, *Lecture Notes on Electron Correlation and Magnetism* (World Scientific, Singapore, 1999)
2. K. Yamada, *Electron Correlation in Metals* (Cambridge University Press, Cambridge, 2004)
3. V. Anisimov, Y. Izyumov, *Electronic Structure of Strongly Correlated Materials* (Springer, Berlin, 2010)
4. A.M. Oleś, J. Phys.: Condens. Matter **24**, 313201 (2012)
5. D. Gotfryd, E. Pärskke, K. Wohlfeld, A.M. Oleś, Condens. Matter **5**, 53 (2020)
6. D. Gotfryd, E.M. Pärskke, J. Chaloupka, A.M. Oleś, K. Wohlfeld, Phys. Rev. Res. **2**, 013353 (2020)
7. M.C. Arnesen, S. Bose, V. Vedral, Phys. Rev. Lett. **87**, 017901 (2001)
8. S.C. Benjamin, S. Bose, Phys. Rev. Lett. **90**, 247901 (2003)
9. G. Vidal, J.I. Latorre, E. Rico, A. Kitaev, Phys. Rev. Lett. **90**, 227902 (2003)
10. L. Amico, R. Fazio, A. Osterloh, V. Vedral, Rev. Mod. Phys. **80**, 517 (2008)
11. N. Laflorencie, Phys. Rep. **646**, 1 (2016)
12. K.I. Kugel, D.I. Khomskii, Sov. Phys. Usp. **25**, 231 (1982)
13. M.E. Amendola, A. Romano, C. Noce, Phys. B **479**, 121 (2015)
14. A.M. Oleś, Phys. Rev. B **23**, 271 (1981)
15. M.J. Rozenberg, Phys. Rev. B **55**, R4855 (1997)
16. J.E. Han, M. Jarrell, D.L. Cox, Phys. Rev. B **58**, R4199 (1998)
17. Y. Imai, N. Kawakami, J. Phys. Soc. Jpn. **70**, 2365 (2001)
18. C. Noce, A. Romano, Phys. Stat. Sol. A **251**, 907 (2014)
19. E. Dagotto, T. Hotta, A. Moreo, Phys. Rep. **344**, 1 (2001)
20. M. Cuoco, C. Noce, Phys. Rev. B **65**, 205108 (2002)
21. M.E. Amendola, C. Noce, J. Phys.: Condens. Matter **18**, 8345 (2006)
22. P.W. Anderson, Phys. Rev. **79**, 350 (1950)
23. P.W. Anderson, Phys. Rev. **115**, 2 (1959)
24. J.B. Goodenough, Phys. Rev. **79**, 564 (1955)
25. J.B. Goodenough, J. Phys. Chem. Solids **6**, 287 (1958)
26. J.J. Kanamori, Phys. Chem. Solids **10**, 87 (1959)
27. P.W. Anderson, in *Magnetism*, G.T. Rado, H. Suhl (eds.), vol. 1, Chapter 2 (Academic Press, New York, 1963)
28. D.I. Khomskii, Phys. Scr. **72**, CC8 (2005)